

Original Article

Validation of MYC and BCL6 rapid break apart digital fluorescence in situ hybridization assays for clinical use

Michael Liew¹, Leslie Rowe¹, Kristina Moore¹, Emily Aston¹, Kathryn O'Brien¹, Maria Longhurst¹, Jason Kenney¹, Marshall Priest¹, Wenhua Zhou¹, Diane Wilcock¹, Anton Rets^{1,2}, Rodney Miles^{1,2}

¹ARUP Institute for Clinical and Experimental Pathology®, Salt Lake, UT 84108, USA; ²Department of Pathology, University of Utah School of Medicine, Salt Lake City, UT 84132, USA

Received November 29, 2022; Accepted March 29, 2023; Epub April 15, 2023; Published April 30, 2023

Abstract: Objective: Detection of gene rearrangements in *MYC* (a family of regulator genes and proto-oncogenes) and human B-cell lymphoma 6 (*BCL6*) using fluorescence *in situ* hybridization (FISH) are important in the evaluation of lymphomas, in particular diffuse large B-cell lymphoma (DLBCL) and Burkitt lymphoma. Our current clinical *MYC* and *BCL6* FISH workflow involves an overnight hybridization of probes with digital analysis using the GenASIs Scan and Analysis instrument (Applied Spectral Imaging). In order to improve assay turnaround time SureFISH probes were validated to reduce the hybridization time from 16 hours down to 1.5 hours. Methods: Validation was a four-phase process involving initial development of the assays by testing new probes in a manual protocol, and cytogenetic studies to confirm the probe specificity, sensitivity, and localization. In the next phase, the assays were validated as a manual assay. The third phase involved development of the digital FISH assays by testing and optimizing the GenASIs Scan and Analysis instrument. In the final phase, the digital FISH assays were validated. Results: Cytogenetic studies confirmed 100% probe sensitivity/specificity, and localization patterns. Negative reference range cutoffs calculated from 20 normal lymph nodes using the inverse of the beta cumulative probability density function (Excel BETAINV calculation) were 11% inclusive for both manual and digital *MYC* and *BCL6* assays. There was 100% concordance between the manual and digital methods. The shortened hybridization time decreased the overall workflow time by 14.5 hours. Conclusions: This study validates the use of the SureFISH *MYC* and *BCL6* probes on formalin fixed paraffin embedded (FFPE) tissue sections using a hybridization time of 1.5 hours that shortened the overall workflow by 14.5 hours. The process described also provides a standardized framework for validating digital FISH assays in the future.

Keywords: GenASIs analysis system, digital pathology

Introduction

In humans, *MYC* is a family of regulator genes and proto-oncogenes named after an oncogene identified in the avian virus *Myelocytomatosis* to which it is also homologous [1]. This family, which is a target for cancer treatment [2-4], includes 3 members: c-*MYC* (*MYC*), l-*MYC* (*MYCL*) and n-*MYC* (*MYCN*). The *MYC* gene located at chromosome 8q24 encodes a 439 amino acid transcription factor [5-7]. Under normal circumstances, *MYC* protein has a key role in regulating cell growth [8]. In a setting of a neoplastic process, including several lymphomas, *MYC* expression is often upregulated [9-12]. In particular, Burkitt lymphoma demonstrates rearrangements occurring between *MYC* and immunoglobulin (IG) heavy chain (*IGH*, chromosome 14q32), kappa light

chain (*IGK*, chromosome 2p11), or lambda light chain (*IGL*, chromosome 22q11) [13-15]. *MYC* translocations with non-IG partners occurs in other high-grade B-cell lymphomas (BCL) including diffuse large BCLs (DLBCLs), and a subset of large BCLs with features intermediate between DLBCL and Burkitt lymphoma [13, 14, 16, 17].

The B-cell lymphoma 6 (*BCL6*, chromosome 3q27), encodes a 706 amino acid protein, and is known as a specific repressor transcription factor [18]. *BCL6* is commonly rearranged in 20-40% of DLBCLs, where it can have IG and non-IG gene partners [19-22]. A subset of DLBCLs previously defined as DLBCL/high-grade B-cell lymphoma with *MYC* and *BCL2* rearrangements (DLBCL/HGBL-*MYC*/*BCL2*) can also have *BCL6* rearrangements

[23]. These types of lymphoma with two or more gene rearrangements (double hit or triple hit lymphomas) tend to have an aggressive clinical course and show a poor response to chemotherapy [24-27].

The prognostic value of the *MYC* and *BCL6* rearrangement necessitates clinical testing of their presence in a subset of B-cell lymphoproliferative disorders. One of the most common tests performed for this purpose is fluorescent in-situ hybridization (FISH) on formalin-fixed paraffin-embedded tissue (FFPE) samples. As an alternative to “manual” analysis and counts of the FISH probe patterns, there are several digital capture and analysis systems available. Our laboratory has published several studies using the GenASIs digital system [28, 29]. Recently, GenASIs has undergone major hardware and software upgrades since those studies were published. Among those upgrades were (1) A higher resolution camera for image capture (5MP); (2) Bright field capture was incorporated into the system optimizing the workflow as slide images no longer need to be converted from a different format to be recognized by the GenASIs system. The software has been improved by incorporating automatic FISH image capture from a single starting point.

In addition to the digital system upgrades, we aimed to improve the assay turnaround time. This was achieved by changing our current probes to SureFISH probes (Agilent Technologies, Santa Clara, CA, USA), which allowed us to shorten our hybridization process from 16 hours to 1.5 hours.

The aim of this study was to validate the SureFISH MYC and BCL6 break apart probes on FFPE samples using a 1.5 hour hybridization protocol and digital analysis. The overall process includes the validation of the new probe by manual FISH analysis first. This step provides a “gold standard” which can also serve as a “back-up” procedure in case the digital system is not available. Here we report our observations developing *MYC* and *BCL6* FISH testing with new probes.

Materials and methods

Cytogenetic analysis - probe localization, sensitivity, and specificity analysis

To ensure that the investigated SureFISH MYC and SureFISH BCL6 probes (Agilent Techno-

logies) perform according to manufacturer's specifications, we performed initial cytogenetic studies. These included (1) a probe localization study, (2) probe sensitivity analysis and (3) probe specificity analysis. The above-mentioned studies were conducted on metaphase spread slides. Metaphase spread slides were prepared from a pooled sample derived from 5 normal male individuals who were referred to ARUP for routine cytogenetic testing.

Metaphase slides were aged either by heating at 56°C for 30 minutes then dehydrated through a series of ethanol washes with increasing concentrations (70%, 85% and 100%) (Thermo Fisher Scientific, Waltham, MA, USA) denatured in 70% formamide (VWR Scientific, Radnor, PA)/2XSSC (Abbott Molecular, Des Plaines, IL, USA) for 5 minutes at 73°C, then dehydrated through another series of ethanol washes (70%, 85% and 100%). Probes were prepared according to manufacturer's instructions, and hybridized to the metaphase slides for 16 hours at 37°C. Following hybridization, the FISH slides were washed first using 0.4XSSC/0.3% NP-40 (Abbott Molecular) at 73°C for 2 mins followed by 2XSSC/0.1% NP-40 at room temperature for 1 minute and air dried. Finally, DAPI II counterstain (Abbott Molecular) was added and the slides were cover slipped and analyzed using an epifluorescence microscope.

FFPE samples

FFPE samples from 50 patients were analyzed using the SureFISH MYC probe. FFPE samples from 40 patients were analyzed using the SureFISH BCL6 probe. Samples were submitted to ARUP for routine hematopathology FISH analysis and selected for this study based on being positive or negative for a MYC or BCL6 rearrangement. This specific study was reviewed by the University of Utah Institutional Review Board (IRB) and granted exempt status, approval number: IRB_00158817. Informed consent for these samples was waived by the IRB.

In addition to sections for FISH studies, H&E stained slides were also performed to confirm the presence of the lesional tissue and identifying the area of interest to be analyzed by the imaging system. The H&E slides are scanned using GenASIs Scan and Analysis instrument (Applied Spectral Imaging, Carlsbad, CA, USA). This is an updated version of a digital FISH

Rapid digital MYC and BCL6 FISH assays

Table 1. Signal pattern definitions

Criteria	Definition
Negative	nF (n≥2)
Rearranged	1F/1G/1R
	1F/1G/nR, (n≥2)
	1F/nG/1R, (n≥2)
	xF/nG/nR, (x>1, n≥1)
	nG/nR, (n≥2)
	nG/1R (n≥2)
Not informative or Atypical	1G/nR (n≥2)
	nF/nG, (n≥1)
	nF/nR, (n≥1)
	1F
	nG, (n≥1)
	nR, (n≥1)
	1G/1R

F = fusion; R = Red, G = Green.

image capture and analysis system we have described previously [28]. Scanning of bright field images has been added to the system, so that every step of image acquisition and analysis can be performed by the same system, which optimized the workflow. As described previously, the digitized H&E slide is used for tumor annotation and alignment with a digital DAPI pre-scan of the FISH slide for accurate transferal of regions of interest.

Fluorescence in situ hybridization

Four-micron unstained FFPE sections were used for FISH analysis. The 8q24 MYC rearrangement was detected using the SureFISH MYC BA P20 break apart probe. The 3q27 BCL6 rearrangement was detected using the SureFISH BCL6 BA P20 break apart probe. FISH slides were pretreated using the PT Link (Agilent Technologies) and washed using a VP2000 Processor (Abbott Molecular) according to each manufacturer's instructions. The SureFISH probes (0.5 ul) were mixed with IQFISH Fast Hybridization buffer (9.5 ul, Agilent Technologies). Hybridizations were carried out on ThermoBrite Systems (Abbott Molecular) using a 10-minute denaturation at 66°C followed by a 90-minute hybridization at 45°C. Post-hybridization washes were carried out on a VP2000 Processor according to manufacturer instructions. Upon completion of washing, slides were mounted using VECTASHIELD® (Vector Labs, Burlingame, CA, USA) according

to manufacturer's instructions and kept in the dark for 15 minutes, then analyzed. Slides that were analyzed manually were read on epifluorescence microscopes equipped with the appropriate filters. Slides that were analyzed digitally were loaded onto the GenASIS Scan and Analysis instrument for a DAPI pre-scan for tissue matching and eventual FISH image capture and analysis.

Reference range, accuracy, & precision

A reference range for the SureFISH probes was defined using 20 samples of non-neoplastic lymphoid tissue. Accuracy was assessed by comparing the SureFISH probe results to the current ARUP clinical FISH assay using 20 negative samples and 20 positive samples for the MYC assay and 10 negative samples and 10 positive samples for the BCL6 assay. Assay precision was assessed using 3 replicates from 3 samples. For intra-assay precision the 3 replicate samples were run at the same time. For inter assay precision, the 3 replicate samples were run on 3 different days. For the digital FISH assays, inter-reader precision was also evaluated. This was assessed using 3 different readers who read the same digital FISH images from each of 3 different samples.

Additional performance assessments

Additional performance assessments of the SureFISH probes on manual FISH were evaluated. Due to the volume of FISH testing performed at the ARUP laboratory, 10 ThermoBrite instruments are available for hybridizations. Sections from the same control block that contained rearranged and non-rearranged tissue were tested across all the ThermoBrite instruments to validate them. To make the workflow as efficient as possible we also evaluated the SureFISH probes' stability by pre-mixing them with hybridization buffer and freezing the aliquots. The aliquots were tested fresh, and after each of four freeze-thaw cycle. To ensure that there was no signal variation caused by section thickness, 3 µm and 5 µm sections were tested.

Manual FISH scoring

Two independent reviewers scored FISH slides. Each reviewer enumerated one-hundred cells. All signal patterns were included in the count with the exception of nuclei showing signals of

Rapid digital MYC and BCL6 FISH assays

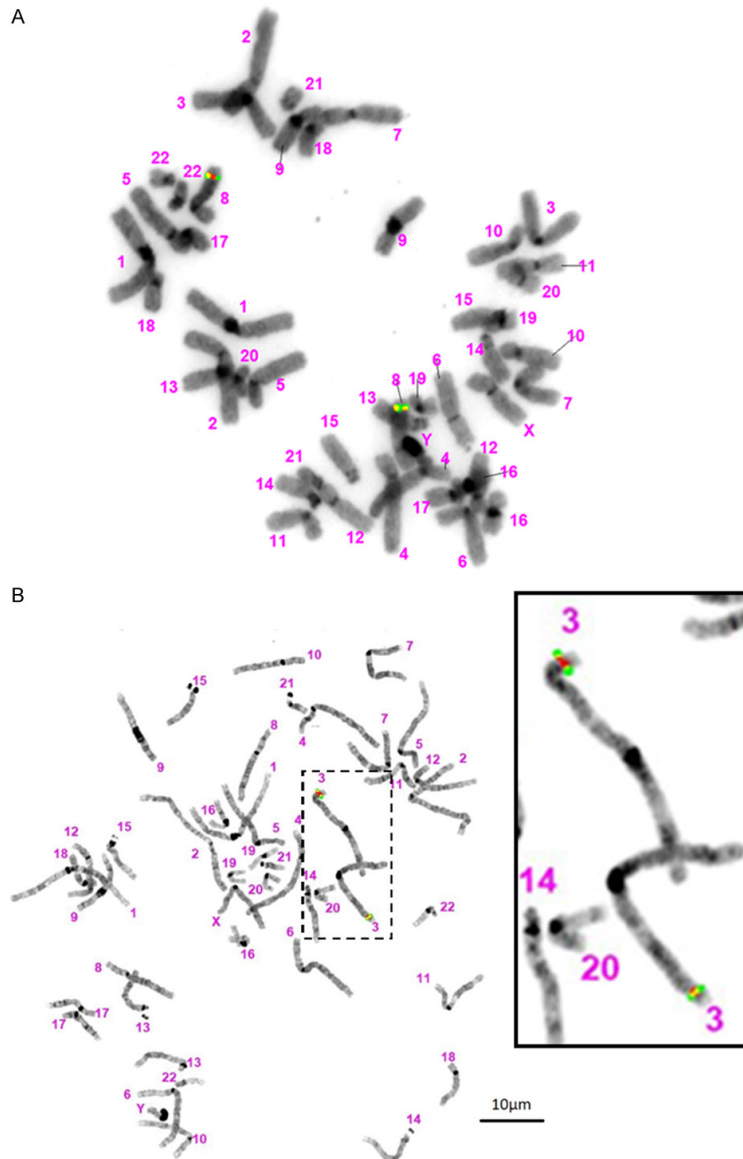


Figure 1. Probe localization of SureFISH MYC (A) and BCL6 (B) probes to pooled male normal human metaphase spreads. For the BCL6 probe, the inset image from dashed rectangle shows probe binding in greater detail. Images were acquired at 60× magnification. A scale bar for both images is shown in (B).

only one probe color and nuclei with only one single fusion, as these findings generally represent either truncation or poor hybridization. See **Table 1** for list of signal pattern definitions.

The more common rearrangement partners for MYC [30] and BCL6 [19, 31, 32] are located on the separate chromosomes, so it would be expected that a broken apart signal (separate orange-red and green) was quite wide. Thus, in

order to be considered being “broken apart” the red and green signals need to be greater than 2 signal widths apart from each other. Sometimes, signal patterns that differ from the classical alterations can be observed in lymphomas. These type of signal patterns are defined as atypical or non-informative, because they can arise both due to a genetic alteration and possibly due to technical artifacts, such as “crush” artifact or signal overlap, or other biological reasons, such as cell cycle phase. The atypical signal patterns are not normally counted during analysis but are noted if they occur frequently.

Data analysis

Probe sensitivity is defined as the number of times that the probe hybridizes to the correct chromosomal location with the expected probe signal [33]. Forty loci (typically 20 metaphase cells) are analyzed. Probe specificity is defined as the number of times that the probe hybridizes to the correct chromosomal location in 40 loci. In both cases, if sensitivity is less than 100%, a total of 100 loci are scored.

Reference range cutoffs were developed based on results obtained from normal lymphoid tissue (primarily non-neoplastic lymph nodes). Cutoffs for manual FISH scoring were calculated using the Microsoft Excel BETAINV function (95% confidence level, average false positive cells + 1, 100 cells analyzed).

Digital FISH counts are sorted using the same definitions for manual FISH counts. However, digital FISH counts using the GenASIs Scan and Analysis instrument are limited by fields of view and not by number of cells counted, so counts

Rapid digital MYC and BCL6 FISH assays

Table 2. Reference range results for the manual SureFISH MYC and B-cell lymphoma 6 (BCL6) assays

Sample #	MYC rearranged (%)			BCL6 rearranged (%)		
	Scorer 1	Scorer 2	Average	Scorer 1	Scorer 2	Average
VAL-01	0	2	1	2	0	1
VAL-02	1	1	1	0	2	1
VAL-03	1	1	1	0	0	0
VAL-04	0	1	0.5	0	0	0
VAL-05	0	0	0	1	3	2
VAL-06	0	2	1	0	0	0
VAL-07	0	1	0.5	0	0	0
VAL-08	0	1	0.5	1	0	0.5
VAL-09	1	1	1	0	0	0
VAL-10	0	2	1	0	0	0
VAL-11	1	1	1	1	9	5
VAL-12	1	3	2	0	0	0
VAL-13	1	2	1.5	0	0	0
VAL-14	2	1	1.5	0	0	0
VAL-15	1	0	0.5	0	2	1
VAL-16	1	0	0.5	1	6	3.5
VAL-17	2	0	1	2	3	2.5
VAL-18	1	2	1.5	0	5	2.5
VAL-19	1	1	1	1	0	0.5
VAL-20	0	0	0	0	1	0.5
BETAINV		(0.95, 3, 100)	6.0		(0.95, 6, 100)	9.8

Rearranged counts are the number observed out of a total of 100. Cutoffs were calculated from the highest average count.

were limited to exactly 100 by deleting acquired cells starting from the last one listed.

Results

Cytogenetics studies

Probe sensitivity and specificity measurements for the SureFISH MYC and BCL6 probes were 100%. Probe localization analysis confirmed that the SureFISH MYC probe hybridized to the 8q24 region, and that the SureFISH BCL6 probe hybridized to the 3q27 region (**Figure 1**).

Manual FISH

The SureFISH MYC and BCL6 probes provided FISH images of FFPE sections with bright signals and low background. This reduced the hybridization turnaround time from 16 hours to 1.5 hours. Twenty non-neoplastic lymphoid tissue samples were used for calculating the reference range for both the manual SureFISH MYC and BCL6 validations (**Table 2**). The cutoffs calculated from the manual FISH reference range results for MYC and BCL6 were 7% and

10% (inclusive), respectively. However, to prevent possible false positives in negative cases with crush artifact, truncation effect, and other suboptimal nuclear morphology that is known to occur in FFPE FISH cases, both cutoffs were raised to 11%, which is similar to cutoffs currently used clinically by ARUP for MYC and BCL6 and would make the workflow simpler. The manual SureFISH MYC and BCL6 assays were 100% concordant with the current clinical FISH assays (**Tables 3, 4**). Qualitative results (rearranged vs non-rearranged) remained the same for all slides for intra-assay and inter-assay precision. Qualitative results across the 10 Thermobrite instruments were in 100% agreement (data not shown). No deterioration in signal or background quality was noticed in the pre-mixed probe mixtures after 4 freeze thaw cycles. No variation in signal patterns or qualitative results was noticed when comparing 5 μ m and 3 μ m sections.

Digital FISH

Results for the digital FISH were similar to the results from the manual FISH. The same twenty

Rapid digital MYC and BCL6 FISH assays

Table 3. Manual SureFISH MYC qualitative accuracy results

Sample #	Clinical MYC result	SureFISH MYC result
MVAL-01	NEG	NEG
MVAL-02	NEG	NEG
MVAL-03	POS	POS
MVAL-04	NEG	NEG
MVAL-05	NEG	NEG
MVAL-06	NEG	NEG
MVAL-07	NEG	NEG
MVAL-08	NEG	NEG
MVAL-09	POS	POS
MVAL-10	NEG	NEG
MVAL-11	NEG	NEG
MVAL-12	NEG	NEG
MVAL-13	NEG	NEG
MVAL-14	NEG	NEG
MVAL-15	POS	POS
MVAL-16	POS	POS
MVAL-17	NEG	NEG
MVAL-18	NEG	NEG
MVAL-19	NEG	NEG
MVAL-20	NEG	NEG
MVAL-21	NEG	NEG
MVAL-22	NEG	NEG
MVAL-23	NEG	NEG
MVAL-24	NEG	NEG
MVAL-25	POS	POS
MVAL-26	POS	POS
MVAL-27	POS	POS
MVAL-28	POS	POS
MVAL-29	POS	POS
MVAL-30	POS	POS

non-neoplastic lymphoid tissue samples were used for calculating the reference range for the digital SureFISH MYC and BCL6 validations (**Table 5**). The cutoffs calculated from the digital FISH reference range results for MYC and BCL6 were both 6% (inclusive). Similar to the manual FISH, to prevent possible false positives in negative cases, both cutoffs were raised to 11%. The digital SureFISH MYC and BCL6 assays were 100% concordant with the manual SureFISH assays (**Table 3**). Representative SureFISH MYC and BCL6 images are shown in **Figure 2**. Qualitative results (rearranged vs non-rearranged) remained the same for all slides for intra-assay, inter-assay and between reader precision.

Table 4. Manual SureFISH BCL6 qualitative accuracy results

Sample #	Clinical BCL6 result	SureFISH BCL6 result
B6VAL-01	NEG	NEG
B6VAL-02	NEG	NEG
B6VAL-03	NEG	NEG
B6VAL-04	NEG	NEG
B6VAL-05	NEG	NEG
B6VAL-06	NEG	NEG
B6VAL-07	NEG	NEG
B6VAL-08	NEG	NEG
B6VAL-09	NEG	NEG
B6VAL-10	NEG	NEG
B6VAL-11	POS	POS
B6VAL-12	POS	POS
B6VAL-13	POS	POS
B6VAL-14	POS	POS
B6VAL-15	POS	POS
B6VAL-16	POS	POS
B6VAL-17	POS	POS
B6VAL-18	POS	POS
B6VAL-19	POS	POS
B6VAL-20	POS	POS

Discussion

Changing our current workflow by switching to the SureFISH MYC and BCL6 probes resulted in a significant improvement of the current workflow by decreasing the hybridization time by (14.5 hours, a 90% reduction). In addition, the SureFISH probes provided good FISH images with bright signals and low background. The current configuration of the GenASIs Scan and Analysis instrument has also led to improvements in the workflow. The ability to image bright field and FISH images on the same system is more efficient than exporting images from one instrument to another, and the higher resolution of the digital camera (5MP vs 1.5MP) improved the image quality.

In our previous work, we described the different signal configurations to determine whether a cell was rearranged or non-rearranged [29]. The original study had a 2-step analysis algorithm, to provide guidance interpreting with the samples that were close to the cutoff, or borderline. However, in our practice, there are not many samples in the borderline category.

Rapid digital MYC and BCL6 FISH assays

Table 5. Reference range results for the digital SureFISH MYC and BCL6 assays

Sample #	MYC rearranged (%)			BCL6 rearranged (%)		
	Scorer 1	Scorer 2	Average	Scorer 1	Scorer 2	Average
VAL-01	0	0	0	0	0	0
VAL-02	0	0	0	0	1	0.5
VAL-03	0	0	0	0	0	0
VAL-04	1	0	0.5	0	0	0
VAL-05	1	2	1.5	0	1	0.5
VAL-06	0	0	0	0	1	0.5
VAL-07	0	2	1	0	0	0
VAL-08	2	1	1.5	0	0	0
VAL-09	1	1	1	0	1	0.5
VAL-10	0	0	0	0	1	0.5
VAL-11	1	1	1	0	0	0
VAL-12	0	3	1.5	2	1	1.5
VAL-13	0	3	1.5	0	0	0
VAL-14	0	1	0.5	0	0	0
VAL-15	1	3	2	0	0	0
VAL-16	0	0	0	0	0	0
VAL-17	0	1	0.5	0	0	0
VAL-18	0	2	1	0	0	0
VAL-19	2	2	2	0	1	0.5
VAL-20	2	0	1	1	0	0.5
BETAINV		(0.95, 2.5, 100)	5.3		(0.95, 3, 100)	6

Rearranged counts are the number observed out of a total of 100. Cutoffs were calculated from the highest average count.

Therefore, in this study we decided to remove the development of the borderline algorithm.

The cutoffs determined from our study were similar to other reports from the literature. In a study that looked at FISH analysis of tissue microarrays of FFPE samples, cutoffs for MYC and BCL6 were 9% and 8% respectively [34]. In a FISH study similar to our own, the authors were able to substantially reduce their experimental process by 12 hours, using Vysis & Zytovision probes and the Panoramic 250 Flash digital microscope platform [35]. Their cutoffs for MYC and BCL6 were 5% and 4% respectively in that study. We did notice that the cutoffs from our digital cutoffs were slightly lower than the manual cutoffs, which could be due to digital images being easier to score.

Although there are many benefits of digital analysis, it does not come without flaws. In our experience, the biggest challenge is the integration of the digital analysis into the existing clinical IT network. The slide images are large files that require separate server space, so

accessing that data through a network with firewalls can be slow. It is very important for the institutions interested in implementing a digital analysis system into a clinical laboratory workflow to ensure the appropriate IT infrastructure is in place.

The digital pathology landscape is continuing to evolve. There are several reviews in the literature summarizing the state of digital pathology with its advantages and challenges [36-38]. ARUP Laboratories has incorporated digital pathology into some workflows as it provides advantages for patient care, together with fiscal responsibilities and regulatory compliance. Together with advances in FISH methodologies, implementation of digital analysis systems introduces significant improvement to the clinical workflow and patient care.

Acknowledgements

The authors would like to acknowledge the technical assistance of the Immunohistochemistry Laboratory FISH bench which includes

Rapid digital MYC and BCL6 FISH assays

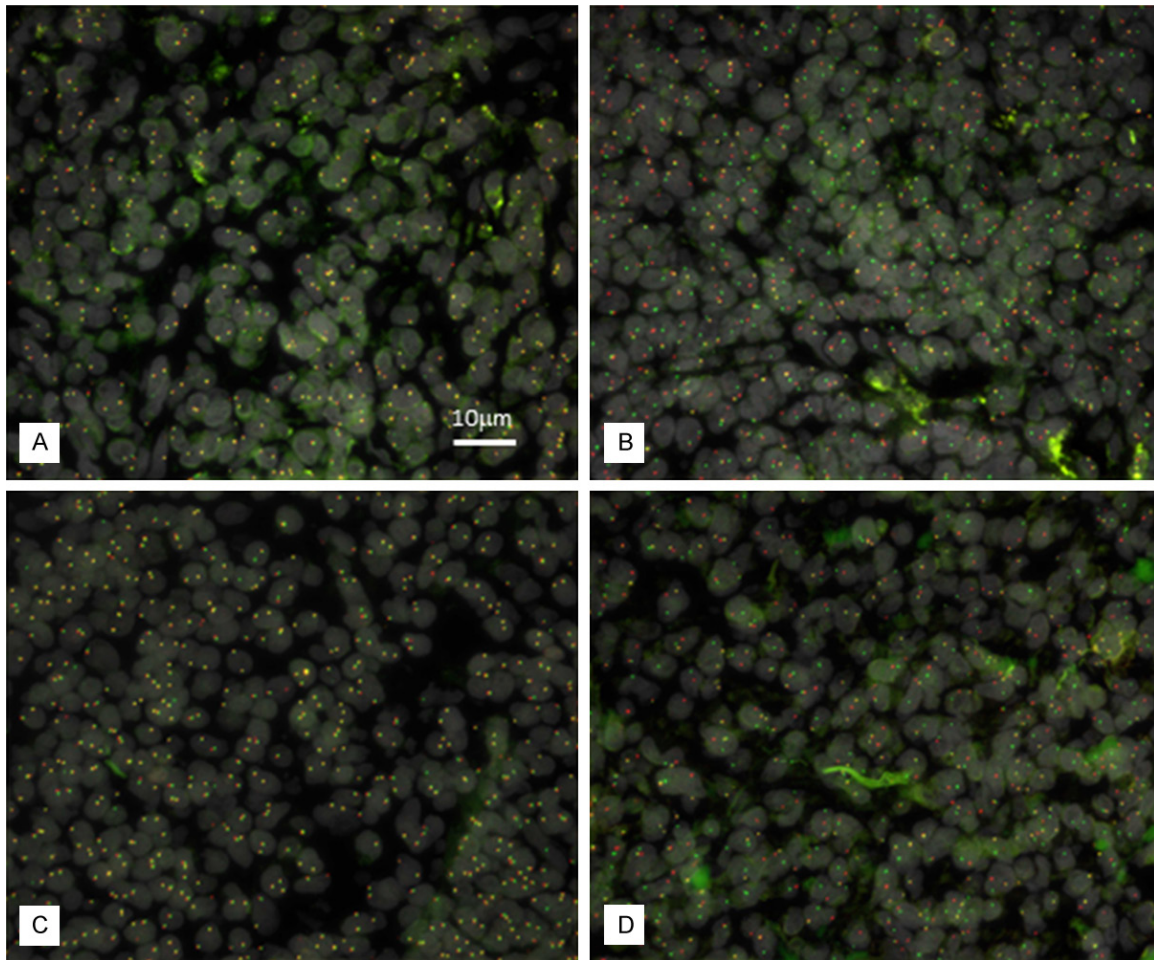


Figure 2. Representative FISH images. MYC (A, MVAL-01) non-rearranged and (B, MVAL-30) rearranged. BCL6 (C, B6VAL-01) non-rearranged and (D, B6VAL-12) rearranged. Images were acquired at 100× magnification. A scale bar for all images is shown in (A).

the following members: Derek Bradshaw, Jesse Burlingame, Richard Davis, Maarika Gering, Meghan Maughan, Prakruti Shaw, Phuong Tran, Olivia Tuono and Nermin Uvezovic. This work was funded by the ARUP Institute for Clinical and Experimental Pathology®.

Disclosure of conflict of interest

None.

Address correspondence to: Michael Liew, ARUP Laboratories, Institute for Clinical and Experimental Pathology, 500 Chipeta Way, Salt Lake, UT 84108-1221, USA. Tel: 801-583-2787 Ext. 2179; E-mail: liewm@aruplab.com

References

[1] Colby WW, Chen EY, Smith DH and Levinson AD. Identification and nucleotide sequence of

a human locus homologous to the v-myc oncogene of avian myelocytomatosis virus MC29. *Nature* 1983; 301: 722-725.

- [2] Baluapuri A, Wolf E and Eilers M. Target gene-independent functions of MYC oncoproteins. *Nat Rev Mol Cell Biol* 2020; 21: 255-267.
- [3] Chen H, Liu H and Qing G. Targeting oncogenic Myc as a strategy for cancer treatment. *Signal Transduct Target Ther* 2018; 3: 5.
- [4] Lombart V and Mansour MR. Therapeutic targeting of “undruggable” MYC. *EBioMedicine* 2022; 75: 103756.
- [5] Dalla-Favera R, Bregni M, Erikson J, Patterson D, Gallo RC and Croce CM. Human c-myc oncogene is located on the region of chromosome 8 that is translocated in Burkitt lymphoma cells. *Proc Natl Acad Sci U S A* 1982; 79: 7824-7827.
- [6] Boerma EG, Siebert R, Kluin PM and Baudis M. Translocations involving 8q24 in Burkitt lymphoma and other malignant lymphomas: a historical review of cytogenetics in the light of to-

Rapid digital MYC and BCL6 FISH assays

- days knowledge. *Leukemia* 2009; 23: 225-234.
- [7] Kato GJ and Dang CV. Function of the c-Myc oncoprotein. *FASEB J* 1992; 6: 3065-3072.
- [8] Dang CV. MYC on the path to cancer. *Cell* 2012; 149: 22-35.
- [9] Dhanasekaran R, Deutzmann A, Mahauad-Fernandez WD, Hansen AS, Gouw AM and Felsher DW. The MYC oncogene - the grand orchestrator of cancer growth and immune evasion. *Nat Rev Clin Oncol* 2022; 19: 23-36.
- [10] Duffy MJ, O'Grady S, Tang M and Crown J. MYC as a target for cancer treatment. *Cancer Treat Rev* 2021; 94: 102154.
- [11] Nitta H. MYC-associated B-cell lymphomas: pathophysiology and treatment. *Rinsho Ketsueki* 2019; 60: 155-164.
- [12] Bisso A, Sabo A and Amati B. MYC in germinal center-derived lymphomas: mechanisms and therapeutic opportunities. *Immunol Rev* 2019; 288: 178-197.
- [13] Brazier RM, Arber DA, Slovak ML, Gulley ML, Spier C, Kjeldsberg C, Unger J, Miller TP, Tubbs R, Leith C, Fisher RI and Grogan TM. The Burkitt-like lymphomas: a Southwest Oncology Group study delineating phenotypic, genotypic, and clinical features. *Blood* 2001; 97: 3713-3720.
- [14] Kanungo A, Medeiros LJ, Abruzzo LV and Lin P. Lymphoid neoplasms associated with concurrent t(14;18) and 8q24/c-MYC translocation generally have a poor prognosis. *Mod Pathol* 2006; 19: 25-33.
- [15] Thomas N, Dreval K, Gerhard DS, Hilton LK, Abramson JS, Ambinder RF, Barta S, Bartlett NL, Bethony J, Bhatia K, Bowen J, Bryan AC, Cesarman E, Casper C, Chadburn A, Cruz M, Dittmer DP, Dyer MA, Farinha P, Gastier-Foster JM, Gerrie AS, Grande BM, Greiner T, Griner NB, Gross TG, Harris NL, Irvin JD, Jaffe ES, Henry D, Huppi R, Leal FE, Lee MS, Martin JP, Martin MR, Mbulaiteye SM, Mitsuyasu R, Morris V, Mullighan CG, Mungall AJ, Mungall K, Mutyaba I, Nokta M, Namirembe C, Noy A, Ogwang MD, Omoding A, Orem J, Ott G, Petrello H, Pittaluga S, Phelan JD, Ramos JC, Ratner L, Reynolds SJ, Rubinstein PG, Sissolok G, Slack G, Soudi S, Swerdlow SH, Traverse-Glehen A, Wilson WH, Wong J, Yarchoan R, Zenklusen JC, Marra MA, Staudt LM, Scott DW and Morin RD. Genetic subgroups inform on pathobiology in adult and pediatric burkitt lymphoma. *Blood* 2022; 141: 904-916.
- [16] Rodig SJ, Vergilio JA, Shahsafaei A and Dorfman DM. Characteristic expression patterns of TCL1, CD38, and CD44 identify aggressive lymphomas harboring a MYC translocation. *Am J Surg Pathol* 2008; 32: 113-122.
- [17] Seegmiller AC, Garcia R, Huang R, Maleki A, Karandikar NJ and Chen W. Simple karyotype and bcl-6 expression predict a diagnosis of Burkitt lymphoma and better survival in IG-MYC rearranged high-grade B-cell lymphomas. *Mod Pathol* 2010; 23: 909-920.
- [18] Albagli-Curiel O. Ambivalent role of BCL6 in cell survival and transformation. *Oncogene* 2003; 22: 507-516.
- [19] Ohno H and Fukuhara S. Significance of rearrangement of the BCL6 gene in B-cell lymphoid neoplasms. *Leuk Lymphoma* 1997; 27: 53-63.
- [20] Willis TG and Dyer MJ. The role of immunoglobulin translocations in the pathogenesis of B-cell malignancies. *Blood* 2000; 96: 808-822.
- [21] Martin-Subero JI, Gesk S, Harder L, Grote W and Siebert R. Interphase cytogenetics of hematological neoplasms under the perspective of the novel WHO classification. *Anticancer Res* 2003; 23: 1139-1148.
- [22] King RL, Hsi ED, Chan WC, Piris MA, Cook JR, Scott DW and Swerdlow SH. Diagnostic approaches and future directions in Burkitt lymphoma and high-grade B-cell lymphoma. *Virchows Arch* 2023; 482: 193-205.
- [23] Alaggio R, Amador C, Anagnostopoulos I, Attygalle AD, Araujo IBO, Berti E, Bhagat G, Borges AM, Boyer D, Calaminici M, Chadburn A, Chan JKC, Cheuk W, Chng WJ, Choi JK, Chuang SS, Coupland SE, Czader M, Dave SS, de Jong D, Du MQ, Elenitoba-Johnson KS, Ferry J, Geyer J, Gratzinger D, Guitart J, Gujral S, Harris M, Harrison CJ, Hartmann S, Hochhaus A, Jansen PM, Karube K, Kempf W, Khoury J, Kimura H, Klapper W, Kovach AE, Kumar S, Lazar AJ, Lazzi S, Leoncini L, Leung N, Leventaki V, Li XQ, Lim MS, Liu WP, Louissaint A Jr, Marcogliese A, Medeiros LJ, Michal M, Miranda RN, Mitteldorf C, Montes-Moreno S, Morice W, Nardi V, Nareish KN, Natkunam Y, Ng SB, Oschlies I, Ott G, Parrens M, Pulitzer M, Rajkumar SV, Rawstron AC, Rech K, Rosenwald A, Said J, Sarkozy C, Sayed S, Saygin C, Schuh A, Sewell W, Siebert R, Sohani AR, Tooze R, Traverse-Glehen A, Vega F, Vergier B, Wechalekar AD, Wood B, Xerri L and Xiao W. The 5th edition of the World Health Organization classification of haematolymphoid tumours: lymphoid neoplasms. *Leukemia* 2022; 36: 1720-1748.
- [24] Copie-Bergman C, Cuilliere-Dartigues P, Baia M, Briere J, Delarue R, Canioni D, Salles G, Parrens M, Belhadj K, Fabiani B, Recher C, Petrella T, Ketterer N, Peyrade F, Haioun C, Nagel I, Siebert R, Jardin F, Leroy K, Jais JP, Tilly H, Molina TJ and Gaulard P. MYC-IG rearrangements are negative predictors of survival in DLBCL patients treated with immunochemotherapy: a GELA/LYSA study. *Blood* 2015; 126: 2466-2474.

Rapid digital MYC and BCL6 FISH assays

- [25] Pedersen MO, Gang AO, Poulsen TS, Knudsen H, Lauritzen AF, Nielsen SL, Klausen TW and Norgaard P. MYC translocation partner gene determines survival of patients with large B-cell lymphoma with MYC- or double-hit MYC/BCL2 translocations. *Eur J Haematol* 2014; 92: 42-48.
- [26] Zhuang Y, Che J, Wu M, Guo Y, Xu Y, Dong X and Yang H. Altered pathways and targeted therapy in double hit lymphoma. *J Hematol Oncol* 2022; 15: 26.
- [27] Cho YA, Hyeon J, Lee H, Cho J, Kim SJ, Kim WS and Ko YH. MYC single-hit large B-cell lymphoma: clinicopathologic difference from MYC-negative large B-cell lymphoma and MYC double-hit/triple-hit lymphoma. *Hum Pathol* 2021; 113: 9-19.
- [28] Liew M, Rowe L, Clement PW, Miles RR and Salama ME. Validation of break-apart and fusion MYC probes using a digital fluorescence in situ hybridization capture and imaging system. *J Pathol Inform* 2016; 7: 20.
- [29] Liew M, Rowe LR, Szankasi P, Paxton CN, Kelley T, Toydemir RM and Salama ME. Characterizing atypical BCL6 signal patterns detected by digital fluorescence in situ hybridization (FISH) analysis. *Ann Lab Med* 2018; 38: 619-622.
- [30] Chong LC, Ben-Neriah S, Slack GW, Freeman C, Ennishi D, Mottok A, Collinge B, Abrisqueta P, Farinha P, Boyle M, Meissner B, Kridel R, Gerrie AS, Villa D, Savage KJ, Sehn LH, Siebert R, Morin RD, Gascoyne RD, Marra MA, Connors JM, Mungall AJ, Steidl C and Scott DW. High-resolution architecture and partner genes of MYC rearrangements in lymphoma with DLBCL morphology. *Blood Adv* 2018; 2: 2755-2765.
- [31] Akasaka H, Akasaka T, Kurata M, Ueda C, Shimizu A, Uchiyama T and Ohno H. Molecular anatomy of BCL6 translocations revealed by long-distance polymerase chain reaction-based assays. *Cancer Res* 2000; 60: 2335-2341.
- [32] Wlodarska I, Mecucci C, Stul M, Michaux L, Pittaluga S, Hernandez JM, Cassiman JJ, De Wolf-Peeters C and Van den Berghe H. Fluorescence in situ hybridization identifies new chromosomal changes involving 3q27 in non-Hodgkin's lymphomas with BCL6/LAZ3 rearrangement. *Genes Chromosomes Cancer* 1995; 14: 1-7.
- [33] JT M. Fluorescence in situ hybridization methods for clinical laboratories. 2nd Edition. Wayne, PA; 2013.
- [34] Horn H, Bausinger J, Staiger AM, Sohn M, Schmelter C, Gruber K, Kalla C, Ott MM, Rosenwald A and Ott G. Numerical and structural genomic aberrations are reliably detectable in tissue microarrays of formalin-fixed paraffin-embedded tumor samples by fluorescence in situ hybridization. *PLoS One* 2014; 9: e95047.
- [35] Chea V, Pleiner V, Schweizer V, Herzog B, Bode B and Tinguely M. Optimized workflow for digitalized FISH analysis in pathology. *Diagn Pathol* 2021; 16: 42.
- [36] Griffin J and Treanor D. Digital pathology in clinical use: where are we now and what is holding us back? *Histopathology* 2017; 70: 134-145.
- [37] Jahn SW, Plass M and Moinfar F. Digital pathology: advantages, limitations and emerging perspectives. *J Clin Med* 2020; 9: 3697.
- [38] Pallua JD, Brunner A, Zelger B, Schirmer M and Haybaeck J. The future of pathology is digital. *Pathol Res Pract* 2020; 216: 153040.